IIETA International Information and Engineering Technology Association
Advancing the World of Information and Engineering

Mathematical Modelling of Engineering Problems
Vol. 12, No. 10, October, 2025, pp. 3435-3446
Journal homepage: http://iieta.org/journals/mmep

Nonlinear Structural Response of Different Web Openings in Composite Beams Reinforced with BFRB Wrapping

Bashar Abid Hamza*, Watheq Naser Hussein, Mohammed Al-Shuraifi

College of Engineering/Al-Musayab, University of Babylon, Al Hillah P.O. Box 4, Iraq

Corresponding Author Email: met.basher.abid@uobabylon.edu.iq

https://doi.org/10.18280/mmep.121010

Received: 17 May 2025
Revised: 13 July 2025
Accepted: 25 July 2025
Available online: 31 October 2025

Keywords:
BFRP, continuous composite beams, finite element model, moment redistribution, nonlinear structural analysis, web openings

ABSTRACT

This study investigates the nonlinear structural behavior of continuous composite beams having different web opening configurations-square, circular, and rectangular under external strengthening using Basalt Fiber-Reinforced Polymer (BFRP) wrapping. Deflection behavior, shear stress distribution, moment redistribution, and ultimate load capacity were evaluated using an analytical approach combined with numerical verification under ultimate loading conditions. An improved analytical model was developed based on the strut-and-tie method and validated with numerical results, achieving high predictive accuracy with a deviation of 5–8%. The results show that the web openings significantly compromise structural performance because they induce stress concentration increasing the deflection and moment redistribution. The most severe effects were found in unstrengthened beams when rectangular opening was used with a redistribution factor (β_{total}), defined as the ratio of redistributed moment to elastic moment, of 0.13 and a decrease in ultimate load capacity of about 10.9%. BFRP wrapping applied brought restoration of structural behavior as load-carrying capacity was restored by up to 9.8% in rectangular-opening beams and the redistribution effect decreased by up to 33.3% in circular-opening beams. BFRP wrapping showed preservation of the ductile behavior of intact beams and stiffness was achieved with the mitigation of adverse effects due to geometric discontinuities. The findings of this study provide practical direction for assessing and strengthening RC beams with web openings, particularly in resilience-oriented retrofitting applications and post-disaster structural evaluations.

1. INTRODUCTION

The up-to-date need for combined architectural and mechanical systems has characteristically resulted in ever-increasing necessity for the integration of web openings within beams. Usually, these openings are offered to allow passage for essential efficacies such as electrical conduits, plumbing, ventilation ducts and communication lines [1]. But their presence as discontinuities greatly affects the internal force distribution and failure mechanisms of beams under ultimate loading conditions [2]. The web openings lead to localized stress concentrations, stiffness reductions, and shear capacity diminutions; all degrade the structural performance and safety of RC members [3-5].

Numerous experimental and numerical studies have evaluated the influence of web openings on the behavior of concrete beams. Abdel-Kareem [6] showed that a shear span rectangular opening had drastic impacts on the capacity as well as the stiffness of RC beams. In the experiment, it was found that when the height increased from 20% to 40% of the depth of the beam, load reduced by 58%, 62%, and 90% typically in comparison with solid reference beams. This confirms that geometry and positioning play critical roles in structural integrity degradation.

Additionally, Sayed [7] simulated RC beams with large rectangular openings located in shear-critical zones. It was found from their research that the beams with unstrengthened openings showed premature brittle shear failures; however, externally bonded Carbon Fiber-Reinforced Polymer Laminates (CFRPs) increased both load capacity and ductility. The other aspect which the authors unfolded was that the effectiveness of CFRP depends on proper anchorage and orientation relative to the principal stress paths.

In like manner, Elansary et al. [8] looked at the bending behavior of RC beams that had rectangular openings close to the supports and showed that unstrengthened beams suffered as much as 43% loss of strength. On the other hand, with CFRP strengthening, these beams gained 95% improvement in load capacity. Such results highlight the important function that fiber-reinforced polymer composites play in offsetting the structural weakness brought about by openings.

The redistribution of internal moments and forces in continuous beams, particularly in webs with openings, is one super important thing that must be considered during structural design. Meng et al. [9] did big tests on continuous RC beams and showed that moment redistribution capacity gets a huge effect from plasticity and geometric discontinuities. Their findings gave a solid push that ignoring redistribution in beams

with openings could make designs unsafe or use material inefficiently.

The shape of web openings has, stress-wise and structurally, an overall reinforcement concrete beam response dependence [10]. Among the most commonly used shapes, square, circular, and rectangular openings, as presented in Figure 1, exhibit distinct behavioral characteristics under loading [11]. Square openings tend to introduce sharp corner which works as stress risers tend to crack initiation and propagation reducing the shear capacity and stiffness of the beam [12]. Circular openings are better since they do not have sharp corners hence there is smooth flow of stresses around the perimeter with low concentration of stresses making them structurally efficient [13, 14]. Rectangular opening beams or exceptionally large aspect ratios compromise beam integrity because they extend the discontinuity over a broad region which strength ductility can severely compromise due to strength reduction coupled with a decrease in ductility material provide supporting role [15]. Studies have shown that beams lose capacity through the unstrengthened introduction of openings, with loss of capacity being greatest in the case of rectangular openings and then square; circular openings are least detrimental. These differences, however, underscore an imperative for customized strengthening solutions when designing or retrofitting beams with such openings.

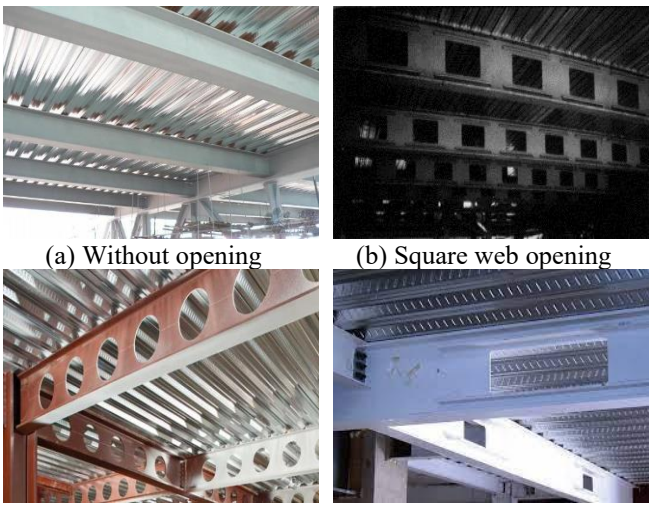

(a) Without opening (b) Square web opening

(c) Circular web opening (d) Rectangle web opening

Figure 1. Typical web opening shapes in continues beams [11]

While large investigations in CFRP [16, 17] and Glass Fiber-Reinforced Polymer (GFRP) [18, 19] have been made as external strengthening approaches, the use of Basalt Fiber-Reinforced Polymer (BFRP) is becoming more popular because it shows good environmental sustainability [20], high thermal stability [21], resistance to corrosion and very good mechanical properties when compared with others reinforcement types [22]. The BFRP is made from volcanic rock which is natural and therefore has low cost and low energy consumption compared to synthetic materials [23, 24]. It provides high tensile strength and a concrete surface match with alkaline environment resistance which are long-term performance requirements factors [25, 26].

Despite these advantages, the gap for the behavior of continuous concrete beams with web openings has hardly been investigated using BFRP wrapping reinforcement. There is not much detailed study on the effect of different shapes of openings (square, circular, rectangular) and configurations of BFRP on nonlinear structural response parameters like mid-span deflection as well as moment redistribution and ultimate shear strength.

This study addresses this gap by creating and validating both analytical and numerical models to explore the nonlinear behavior of continuous RC beams-with and without web openings, with and without BFRP strengthening. Loads, moment redistribution factors, and deformation characteristics are key performance indicators considered in the analysis. The study highlights how much BFRP wrapping mitigates the ill-effects introduced by the web openings simultaneously it would be secured under ultimate load conditions every time a web opening is present. Results help improve practical understanding on combined geometry and composite reinforcement for structural engineers to consider in new designs as well as retrofit applications.

2. SPECIMEN DESIGN

To enable a complete comparative study regarding the impacts of web opening shapes and strengthening with BFRP on the performance of continuous composite beams, a total of eight full-scale specimens were designed and manufactured. The design parameters were taken from relevant earlier research so that adaptation would bring consistency with the established experimental methods and thus make possible higher validity for comparisons.

Specimens were classified into two primary categories, unstrengthened and BFRP-strengthened. The former comprises four beams, which are used in this experiment. The first beam was incorporated as a solid control specimen having no web openings and is named Composite Beam without opening (WCB). The other three beams fall within different geometries of web opening at the same location along the span: square openings (200 mm × 200 mm) in Composite Beam with Square opening (SCB); circular openings (200 mm diameter) in Composite Beam with Circular opening (CCB); and rectangular openings (400 mm × 200 mm) in Composite Beam with Rectangular opening (RCB). Corresponding BFRP-strengthened versions of each beam were prepared and labeled Composite Beam without opening strengthened with BFRP (BWCB), Composite Beam with Square opening strengthened with BFRP (BSCB), Composite Beam with Circular opening strengthened with BFRP (BCCB), and Composite Beam with Rectangular opening strengthened with BFRP (BRCB) respectively. These specimens were externally wrapped by BFRP sheets at the web openings as well as other major regions to raise their load-carrying capacities and decrease stress concentrations.

Each beam was made as a full composite structure having two equal spans of 5000 mm. The steel section applicable to all specimens was a Q235B hot-rolled H-section beam of 300 mm height, flange width 125 mm, and web thickness and flange thickness of 6 mm and 10 mm respectively. To complete the composite cross-section, a concrete slab cast on top of the steel beam measured 1000 mm in width and 110 mm in thickness. At the interface between the steel beam and concrete slab, standard welded shear studs of diameter 19 mm uniformly spaced at 100 mm intervals were provided to ensure full shear interaction and composite action.

Penetrations were strategically placed to mimic realistic scenarios of service integration, e.g., HVAC or piping

penetrations. For each span, three penetrations were provided at one-third span (L/3), mid-span (L/2), and three-quarters span (3L/4) with the same placement for all specimens to allow easy comparison.

All beams were molded using C30-grade concrete as per normal construction guidelines. The concrete slabs had reinforcement with Ø8 mm deformed bars placed longitudinally and transversely at 100 mm spacing for controlling shrinkage cracks as well as providing reasonable ductility; adequate conditions for the specimens that were strengthened. BFRP sheets were used in the important areas around the openings applied with a superior adhesive, according to normal rules of application and wrapping, onto prepared surfaces.

Balanced two-point static load was used at the center of each sample during test to mimic normal loading situations met in continuous beam structures. This loading setup was picked to create an obvious bending response and enable seeing failure types and stiffness traits under similar conditions.

Table 1. Details of test specimens

Specimen	Opening Size (mm)	Steel Section $h_s \times b_f \times t_w \times t_f$ (mm)	Span Length $L_1 = L_2$ (mm)	Concrete Slab b_c (mm)	h_c (mm)	Flange Reinforcement		BFRP Wrapping
						Longitudinal	Transverse	
WCB	None	300 × 125 × 6 × 10	5000	1000	110	Ø8 @ 100 mm	Ø8 @ 100 mm	No
SCB	$W_o \times h_o$ (200 × 200)	300 × 125 × 6 × 10	5000	1000	110	Ø8 @ 100 mm	Ø8 @ 100 mm	No
CCB	$W_o = h_o$ (200)	300 × 125 × 6 × 10	5000	1000	110	Ø8 @ 100 mm	Ø8 @ 100 mm	No
RCB	$W_o \times h_o$ (400 × 200)	300 × 125 × 6 × 10	5000	1000	110	Ø8 @ 100 mm	Ø8 @ 100 mm	No
BWCB	None	300 × 125 × 6 × 10	5000	1000	110	Ø8 @ 100 mm	Ø8 @ 100 mm	Yes
BSCB	$W_o \times h_o$ (200 × 200)	300 × 125 × 6 × 10	5000	1000	110	Ø8 @ 100 mm	Ø8 @ 100 mm	Yes
BCCB	$W_o = h_o$ (200)	300 × 125 × 6 × 10	5000	1000	110	Ø8 @ 100 mm	Ø8 @ 100 mm	Yes
BRCB	$W_o \times h_o$ (400 ×2 00)	300 × 125 × 6 × 10	5000	1000	110	Ø8 @ 100 mm	Ø8 @ 100 mm	Yes

Note: *h_s is the steel beam's height, b_f is the steel flange's width, t_f is the thickness of the flange, t_w is the steel web's thickness, h_c and b_c are the concrete slab's thickness and width, respectively.

Table 1 presents a detailed summary of the geometric and material characteristics of all test specimens, highlighting opening types, reinforcement details, and BFRP application. The geometrical layout and cross-sectional details of the specimens are further illustrated in Figures 2 and 3.

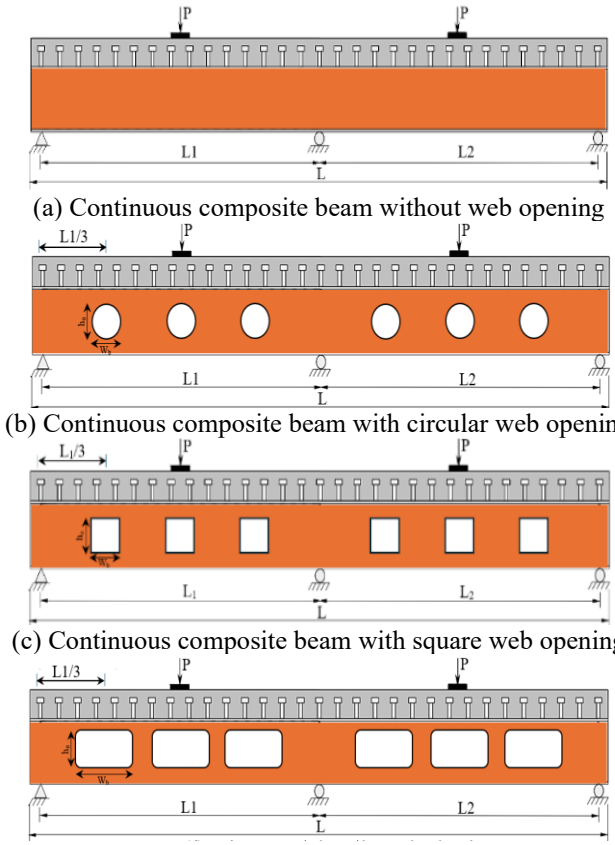

(a) Continuous composite beam without web opening

(b) Continuous composite beam with circular web opening

(c) Continuous composite beam with square web opening

(d) Continuous composite beam with rectangular web opening

Figure 2. Longitudinal geometrical dimensions of the continuous composite beam specimens

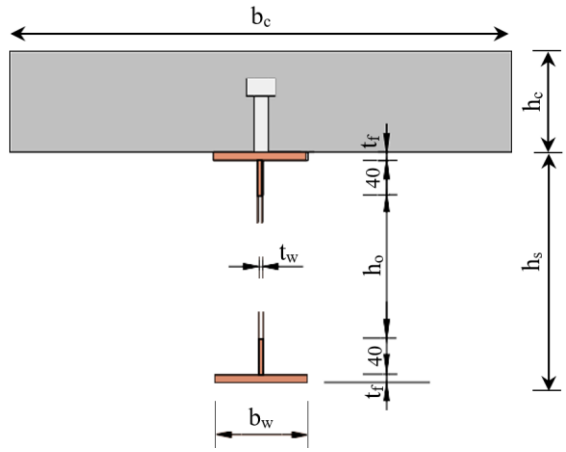

Figure 3. Cross-sectional dimensions of the continuous composite beam specimens

3. MATERIAL PARAMETERS AND MODEL ESTABLISHING

3.1 Concrete properties

In the finite element (FE) simulation, concrete was modeled using the multilinear isotropic strain hardening and multilinear isotropic hardening (MISO) model to accurately reflect its nonlinear behavior under compressive stress [25]. This model is widely adopted for simulating the mechanical response of concrete in structural analyses. The stress–strain relationship is defined according to the characteristic curve shown in Figure 4. The curve incorporates the axial compressive strength f_c, with the strain at peak stress ϵ_0 taken as 0.002 and the ultimate strain ϵ_{cu} set at 0.0033, consistent with previous validated studies [27, 28]. The model effectively captures both the ascending and descending branches of the concrete's behavior, thus providing reliable input for nonlinear finite element analysis of composite members.

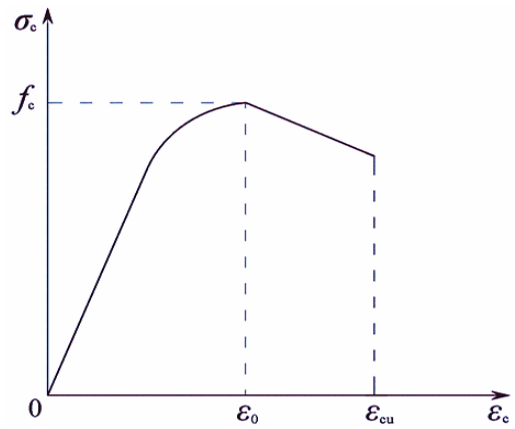

Figure 4. Concrete stress-strain curve

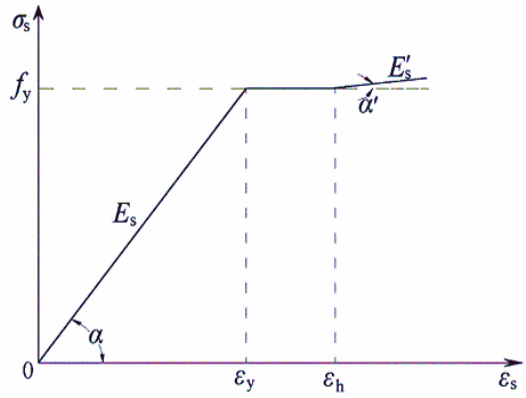

Figure 5. Steel constitutive relationship curve

3.2 Steel properties

For both the Q235B H-section steel and the reinforcement bars, an elastic–plastic constitutive model incorporating a strain-hardening stage was employed. This approach ensures computational stability and enhances the convergence of the nonlinear finite element analysis, particularly under large deformation or post-yield loading conditions. The typical stress–strain behavior is illustrated in Figure 5. The initial modulus of elasticity for steel, E_s, is assumed to be 2.06×10^5 MPa. A secondary modulus $\acute{E}_s$ of 2.06×10^3 MPa, representing the strain-hardening phase, was also adopted based on established literature. The yield strength of the steel components, including both the H-section and reinforcing bars, was determined from material properties reported in prior research [29].

3.3 Stud properties

The shear behavior of the welded studs, serving as the mechanical connectors between the steel beam and concrete slab, was modeled using the empirical load-slip relationship proposed by Ollgaard et al. [30]. This relationship accurately represents the interaction between the two composite materials under load. The uplift resistance of the supports was neglected in this research, as longitudinal sliding at the steel-concrete interface is the primary focus of interest, and because vertical uplift stress does not significantly affect the overall stability of continuous composite beams. To simplify the finite element model and focus exclusively on shear interaction, the longitudinal and transverse freedom variables within the steel beam and concrete floor were coupled.

3.4 BFRP

In this research, BFRP was adopted strengthening method applied along the steel beam flanges. BFRP wrapping has flexural performance enhancement show bending resistance improvement and mitigate local buckling effect on the flanges when loaded application. Considering BFRP for its superior mechanical property's high tensile strength big low weight and corrosion resistance durability solution wherever applicable to increase both structural element's durability and functionality.

The BFRP sheets wrapped around the outer surfaces of the flanges applied at top and bottom flanges of the steel beam. Normally, these regions would see maximum bending stresses, particularly in composite beams where along one way, steel and concrete interact for load transfer. The BFRP wrapping applied here increases tensile strength on steel flanges preventing premature plastic deformation in areas where stress concentrations could occur.

BFRP sheets were bonded using high-strength epoxy adhesive after the surface preparation of steel to ensure an effective bond. The wrapping was done longitudinally along the length of the beam covering flanges to enhance the overall structural integrity of the beam. This application helped in providing additional confinement to the flange areas and thus increased both strength and stiffness for the composite beam.

The BFRP material was used as a longitudinal sheet, matched with the expected main tensile stresses. The main goal was to increase the bending performance of the beam by giving extra resistance to bending and enhancing the capacity to carry load, especially in places where shear and bending forces are highest.

3.5 Establishing the finite element model

The finite element model (FEM) for analyzing the behavior of continuous composite beams was developed using ABAQUS software, ensuring accurate material behavior and structural response. The model was set up to mechanically perform the composite beam specimens, considering all aspects, which include the concrete slab, steel beam, shear connectors, and BFRP reinforcement placed along the steel flanges.

3.5.1 Modeling assumptions

To ensure an efficient and accurate simulation several modeling assumptions were made. The concrete was assumed to be homogeneous and isotropic in compression modeled using the multilinear isotropic strain hardening (MISO) model [31]. This effectively captures nonlinear behavior under loading. Steel sections and reinforcing bars are treated as elastoplastic materials with isotropic strain hardening for reflect their yielding and post-yield characteristics. The BFRP was defined as a linear elastic orthotropic composite with material properties aligned with the fiber orientation. Perfect bonding was assumed between the concrete and steel in areas without shear connectors.

3.5.2 Model geometry and mesh

The continuous composite beam specimen geometry was mirrored in the finite element model designed by the physical specimen. Discrete beam element division was performed with suitable mesh size selection that balances computation efficiency and accuracy. 2D or 3D solid elements for concrete slabs and steel sections were used to model the beam

depending on area interest. Contact elements were used to model interfaces between concrete and steel so that interactions between these two materials can be captured appropriately. BFRP wrapping is modeled as a surface layer on steel flanges which are modeled as shell elements with underlying steel substrate interaction.

A mesh sensitivity analysis was conducted to determine the optimal element size for capturing stress concentrations and load-deflection responses accurately. The beam components were discretized using 3D eight-node linear brick elements with reduced integration (C3D8R) for the concrete and steel, and four-node shell elements (S4R) for the BFRP wrapping. Three mesh densities coarse (50 mm), medium (25 mm), and fine (10–15 mm), were tested. The fine mesh, applied particularly in critical regions such as loading points and the steel and concrete interface, provided a stable and accurate simulation with detailed stress localization and proper deflection behavior.

3.5.3 Boundary conditions and loading

The finite element model was configured with similar boundary conditions to that of the experimental setup. The beam was simply supported at both ends, and mid-span two-point loading was applied symmetrically as per the experiment. The applied loads were uniformly distributed over the two points as per the testing procedure. Symmetric loading ensured that real-life responses would be modeled accurately by the beam under this arrangement.

3.5.4 Material models

To describe the different materials' responses in the composite beam, the model used various constitutive relationships. Concrete was implemented using the MISO model for multilinear isotropic strengthening, which considers the nonlinear stress-strain behavior of concrete. The sections and reinforcing bars were modeled using an elastic-plastic format with a strain-hardening shame to represent the typical stress-strain curve for steel. The BFRP material was modeled by an appropriate composite material model to show its function in improving beam performance.

3.5.5 Shear connectors and BFRP wrapping

Shear connectors were introduced to the model as welded studs, applied in the FEM through special contact elements to represent their interaction between the concrete slab and steel beam. Their load-slip relationship was taken from prior work and implemented to make sure shear forces transfer accurately between the two materials. For BFRP, a layer of shell elements was used over the top and bottom steel flanges to mimic the enhancement provided by reinforcement. The bond between BFRP and steel was modeled using a cohesive zone model representing the effects of adhesive bonding.

3.5.6 Analysis procedure

The FEA was carried out using static, nonlinear analysis to mimic the response of the beam under loading. Nonlinear material behavior, contact interactions, and BFRP strengthening were considered in the simulation. Main outputs from the FEM include load-deflection curve and stress distribution across beam cross-section along with failure modes, whether localized buckling or cracking in concrete slab as shown in Figure 6.

Results from the finite element model were validated with experimental data to ensure accuracy of the simulation. Discrepancies between FEM results and observations in experiments were minimized by refining the mesh and adjusting material models as necessary. Thus, it became possible to develop an understanding of the structural behavior of continuous composite beams, BFRP-reinforced as well as unreinforced.

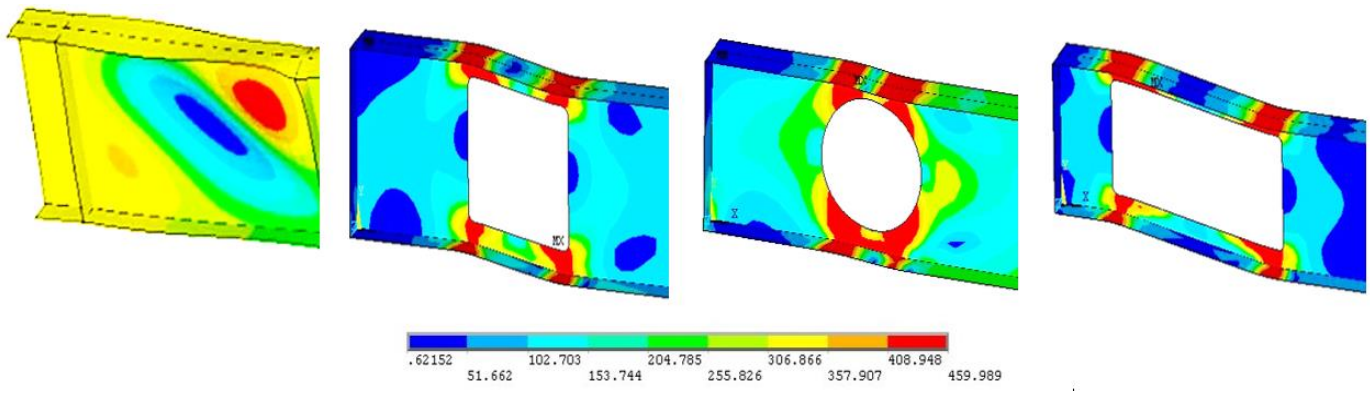

Figure 6. FE model results of selected composite beam

3.5.7 Replication of experimental boundary conditions

The replication of an experimental boundary conditions in numerical model was a critical to ensure the validity of FEM results. The beam was simply supported at both ends which matching the laboratory setup. One support restrained both vertical and lateral movements while the other restrained only vertical movement to allow for thermal expansion and avoid over-constraining the structure. Loading was applied through two concentrated forces at mid-span using rigid loading plates and reference points. Smooth amplitude curve was used for gradually apply the static load which enhanced the convergence of the nonlinear analysis.

4. ANALYTICAL STUDY

The ultimate shear capacity prediction of deep beams has opened vast research areas, especially in those with openings. It led to several methodologies capable of modeling such nonlinear and complex strain flows typical of these structures [32]. Considerably powerful methods for shear capacity prediction have been strut-and-tie models and nonlinear finite element analysis. The former provides an intuitive conception for the highly distributed stress within a structural member by decomposing it into a set of axial actions like a truss system. Concrete struts within the model carry the compressive stresses while reinforcing steel bars act as ties to carry the

tensile stresses. Basalt Fiber Reinforced Polymer will thus be used to support the performance of the entire beam.

Nodal regions are the connections between supports and ties in a brace-and-tie model. The theory of minimum plasticity states that the predicted shear capacity of a brace-and-tie model is consistently lower than the actual capacity of a structure in equilibrium [33-35]. According to Russo [36], one of the most accurate techniques based on the brace-and-tie methodology can accurately predict the ultimate shear capacity of deep beams. This technique considers both vertical and horizontal web shear reinforcement when calculating the total shear strength of the beam.

The boundary conditions for the analytical model are like those for the numerical configuration, which features direct support at both ends of the beam. In addition to two empirical constants that consider the effects of vertical and horizontal web shear reinforcement, the shear capacity prediction formula, as proposed by this methodology, appears in a polynomial estimate of the concrete strength, minimizing the softening coefficient.

The shear capacity V_u of a concrete deep beam, incorporating factors for concrete strength, web reinforcements, and BFRP enhancements, is expressed as:

$$V_u = x \cdot \rho_f \cdot \rho_h \cdot \rho_v \cdot \left(E_s \cdot f_y \cdot \theta \cdot \frac{l}{d}\right) \quad (1)$$

where, x = Nondimensional interpolating function; ρ_f = Ratio of main reinforcement; ρ_h = Ratio of horizontal web shear reinforcements; ρ_v = Ratio of vertical web shear reinforcements; E_s = Modulus of elasticity of steel (200,000 MPa); f_y = Yield strength of steel (MPa); θ = Angle between the strut and the vertical axis; d = Effective depth of the beam; and l = Span length of the beam.

The angle θ between the strut and the vertical axis is determined by:

$$\theta = arctan\frac{V_s}{N_s} \quad (2)$$

where, V_s = Shear force acting on the strut; and N_s = Axial force in the strut.

The coefficient R_o exhibits the effect of openings on concrete strength. It is determined based on the diameter d_o of the opening and its location relative to the load path:

$$R_o \begin{cases} 1.0 & \text{if the opening does not intersect the load path} \\ f(d_o) & \text{if the opening intersects the load path} \end{cases}$$

where, d_o = Diameter of the opening; $f(d_o)$ = Empirical function to be determined based on numerical data.

After considering the effects of load exposure, the final shear capacity is given by:

$$\acute{V_u} = (x \cdot \rho_f \cdot \rho_h \cdot \rho_v) \cdot \left(E_s \cdot f_y \cdot \theta \cdot \frac{l}{d}\right) \cdot \left(R_f \cdot R_o\right) \quad (3)$$

where, R_f = Residual strength factor of concrete post-load exposure (0.4 for 800°C exposure as per Eurocode); and R_o = Coefficient reflecting the effect of openings on concrete strength.

To enhance the prediction accuracy of the proposed model, particularly under combined thermal and geometrical disturbances, three empirical coefficients c_1, c_2 and c_3 were introduced into the formulation (embedded within the factor x). These coefficients govern the contribution of reinforcement ratios and structural geometry to the overall strength equation.

To minimize the variability in the shear capacity prediction, the coefficients c_1, c_2 and c_3 are find out by decreasing the coefficient of variation (COV), which is the ratio of the standard deviation (STD) to the average (AVG) of measured strength of shear values:

$$COV = \frac{STD}{AVG} \quad (4)$$

where, STD = Standard deviation of the numerical shear strength; and AVG = Average of the numerical shear strength

The coefficients c_1, c_2 and c_3 are adjusted to minimize this COV, providing a more accurate prediction for the final shear strength.

The present research aims to predict the ultimate residual shear strength of deep beams after loading. A reduction factor for the concrete strength resulting from loading has been incorporated into the Rousseau technique [36]. According to the approved Rousseau technique standards, a constant value of 0.545 is proposed for the coefficient c_1 for all specimens. Furthermore, values of 0.125 and 0.175 are assigned to the empirical constants c_2 and c_3, which are found by minimizing the shear strength coefficient (COV) across the practical and nominal shear forces. Eq. (3) provides the formula for the ultimate shear capacity of beams subjected to loading. According to the correlations established by Eurocode and numerous published research in the literature, the value of R_f, which represents the ultimate strength factor of concrete after loading, is constant at 0.4. This reduction in strength is incorporated into the final analysis.

The geometry of the specimens in the study dictates that $P_u = 2V_u$, where, V_u represents the shear force. The shear stress v_u is calculated as:

$$v_u = \frac{P_u}{2bd} \quad (5)$$

where, b = Width of the beam; and d = Depth of the beam.

According to Eurocode 2: Design of concrete structures – Part 1-2: General rules, Structural fire design (EN 1992-1-2, 2004), the residual strength of concrete subjected to high temperatures decreases significantly with increasing exposure. For normal strength concrete exposed to 800°C, the compressive strength retention factor is typically in the range of 0.3 to 0.45, depending on the duration of heating and cooling conditions. In this study, a conservative value of $R_f = 0.4$ was adopted to reflect the residual mechanical performance of concrete after thermal degradation, as recommended in the Eurocode. This factor enables realistic estimation of post-fire shear capacity and is consistent with values used in similar thermal degradation models for structural concrete.

The designed approach accurately predicts the ultimate shear capacity of the beams under load, as shown in Table 2. The ultimate shear capacity of the brace and tie model, which is based on the minimum plasticity hypothesis, is often lower than the values found in experimental tests. This result indicates that the proposed analytical model predicts the shear properties of composite beams with slots, both before and after load, with a high degree of accuracy and reliability.

Table 2. Validation of the numerical and analytical results

Specimen ID	Opening	Numerical Pu (kN)	Analytical Pu (kN)	Numerical Shear Vu (MPa)	Analytical Shear Vu (MPa)	Rf	Difference (%)
WCB	No	460	448.2	3.05	2.96	0.974	2.56%
SCB	Yes	420	408.6	2.88	2.8	0.973	2.71%
CCB	Yes	430	418.6	2.95	2.87	0.974	2.65%
RCB	Yes	410	398.7	2.8	2.71	0.973	2.74%
BWCB	No	490	477.3	3.3	3.2	0.974	2.59%
BSCB	Yes	455	442.2	3.1	3	0.972	2.81%
BCCB	Yes	460	446.2	3.18	3.08	0.97	2.99%
BRCB	Yes	450	437.2	3.05	2.95	0.971	2.84%

5. ANALYSIS OF FINITE ELEMENT RESULTS

5.1 Load-deflection curves

The load-deflection response is a major characteristic of the structural performance and ductility of composite beams. An FE analysis was performed to model the behavior of all eight models under two-point loading conditions. Results were obtained at mid-span for each beam and compared with analytical values to validate the numerical model.

Figure 7 shows the load-deflection curves for composite beams, one unstrengthened and the other strengthened with BFRP. All beams showed an initial linear response up to the point of yielding, after which a phase of nonlinearity led to ultimate failure. The FE outcomes were in respectable accord with analytical numbers in meshing both elastic and post-yield behaviors.

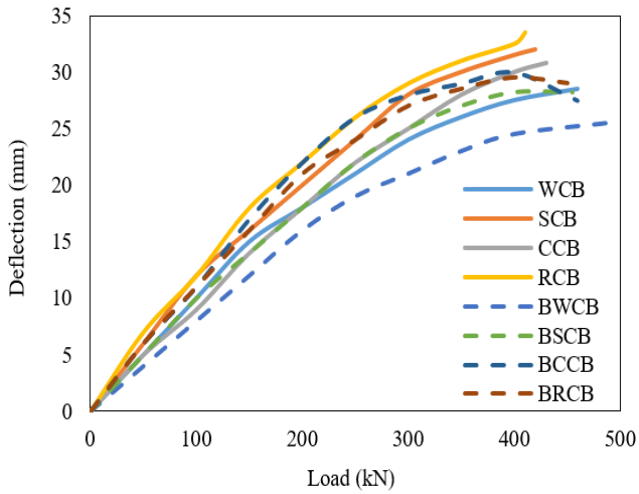

Figure 7. Load-deflection curves of composite beams with varied opening shapes

For the unstrengthened specimens (WCB, SCB, CCB, RCB), web opening presence and geometry played a major role in stiffness as well as ultimate load capacity. Of all the specimens tested, solid control beam (WCB) showed maximum stiffness and load-bearing capacity; on the other hand, rectangular opening specimen (RCB) showed the most marked reduction in both types of capacities-stiffness as well as deflection. The reason for such behavior is stress concentration together with reduced shear transfer area around openings.

The BFRP-strengthened beams (BWCB, BSCB, BCCB, BRCB) gave a contrasting performance. The wrapping of BFRP considerably delayed the local buckling and stress was redistributed around the openings; as a result, the capacity of loads delivered moved to a higher degree along with deflection reduction. Among all strengthened specimens, BWCB beam showed maximum enhancement; however, due to its larger opening, a direct impact was lesser but still significant increase in strength as well as stiffness compared to unstrengthened beam.

The FE-predicted load-deflection curves nearly mirrored the analytical responses, the maximum deviation in peak load being not more than 3%, as also indicated in Table 3. This validates and makes reliable the finite element models developed here in simulating the complex behavior of composite beams both with and without web openings, along with BFRP reinforcement.

Table 3. Load-deflection results of tested models

Specimen ID	Ultimate Load Pu (kN)	MidSpan Deflection Δu (mm)	Initial Stiffness K (kN/mm)
WCB	460	28.5	21.58
SCB	420	32	17.67
CCB	430	30.8	18.71
RCB	410	33.5	16.12
BWCB	490	25.5	25.57
BSCB	455	28.2	21.47
BCCB	460	27.5	22.36
BRCB	450	29	20.18

5.2 Cross-sectional shear distribution

Shear distribution across the depth of composite beams significantly influences the overall behavior, particularly in the presence of web openings. The following paragraphs below analyze and compare the shear stress patterns in specimens with and without web openings under identical loading conditions.

In specimens without web openings (e.g., WCB and BWCB), the shear force is primarily resisted by the steel web. The distribution of shear stress is approximately parabolic, with the maximum shear occurring at the neutral axis and diminishing towards the flanges. The concrete slab contributes marginally to shear resistance but enhances stiffness and prevents local buckling. In the BFRP-strengthened specimen (BWCB), although the web remains unperforated, the BFRP wrapping provides additional stiffness, leading to a more uniform shear distribution and slight reduction in peak shear stresses. This reinforces the web against initial yielding and delays the onset of web buckling.

Specimens with web openings (SCB, CCB, RCB) exhibit a significant alteration in shear distribution. The presence of voids on the web interrupts the natural shear flow, inducing

stress concentrations around the opening edges. The shear is redistributed to the surrounding areas, particularly above and below the openings, resulting in localized high shear zones. SCB and CCB these specimens showed a clear disruption in the central shear flow, with circular openings (CCB) having a smoother redistribution compared to square ones due to the absence of sharp corners. RCB these produced the most severe stress concentrations, especially at the corners, due to their large aspect ratio and sharper stress risers. For BFRP-strengthened beams (BSCB, BCCB, BRCB), the externally bonded fibers confined the stress flow around the openings, reduce stress concentrations, and improved shear capacity. The wrapping redistributed the shear more uniformly around the disturbed region and enhanced the post-yield behavior of the web.

Figure 8 demonstrates the analysis of the beams without web openings and exhibited the most efficient shear stress distribution. The control specimen (WCB) reached a maximum shear stress of 1.2 MPa, following a near-parabolic profile. When strengthened with BFRP (BWCB), the peak stress slightly decreased to 1.1 MPa, and the distribution became more uniform, indicating improved shear performance due to external confinement.

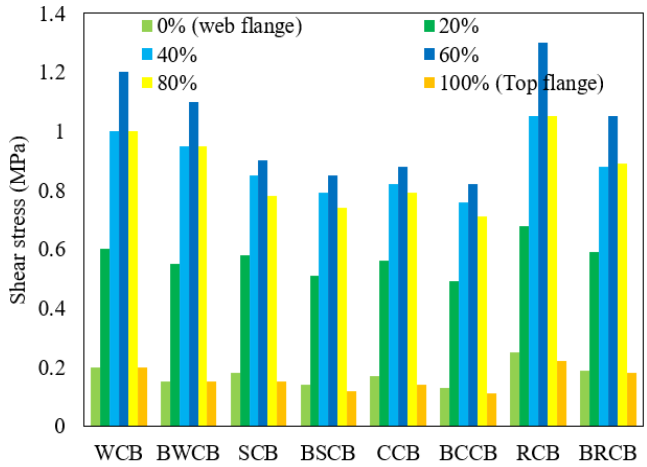

Figure 8. Shear stress distribution along web height at mid-span

Beams with web openings experienced notable reductions in shear efficiency. The square-opening beam (SCB) and circular-opening beam (CCB) showed reduced peak shear stresses of 0.9 MPa and 0.88 MPa, respectively, compared to WCB. Strengthening these specimens with BFRP (BSCB and BCCB) further reduced the peak stresses to 0.85 MPa and 0.82 MPa, respectively, while improving the stress distribution near the openings.

The most severe shear stress concentration occurred in the rectangular-opening specimen (RCB), where the peak shear stress rose to 1.3 MPa due to significant web discontinuity. The application of BFRP in BRCB reduced this peak to 1.05 MPa, reflecting a substantial improvement in stress control despite the large opening.

In conclusion, the results confirm that web openings reduce shear performance, with rectangular shapes being the most critical. However, BFRP wrapping effectively reduces peak shear stresses (by up to 19.2% in the case of RCB to BRCB) and restores more uniform stress distribution, thereby enhancing the structural performance of beams with web perforations.

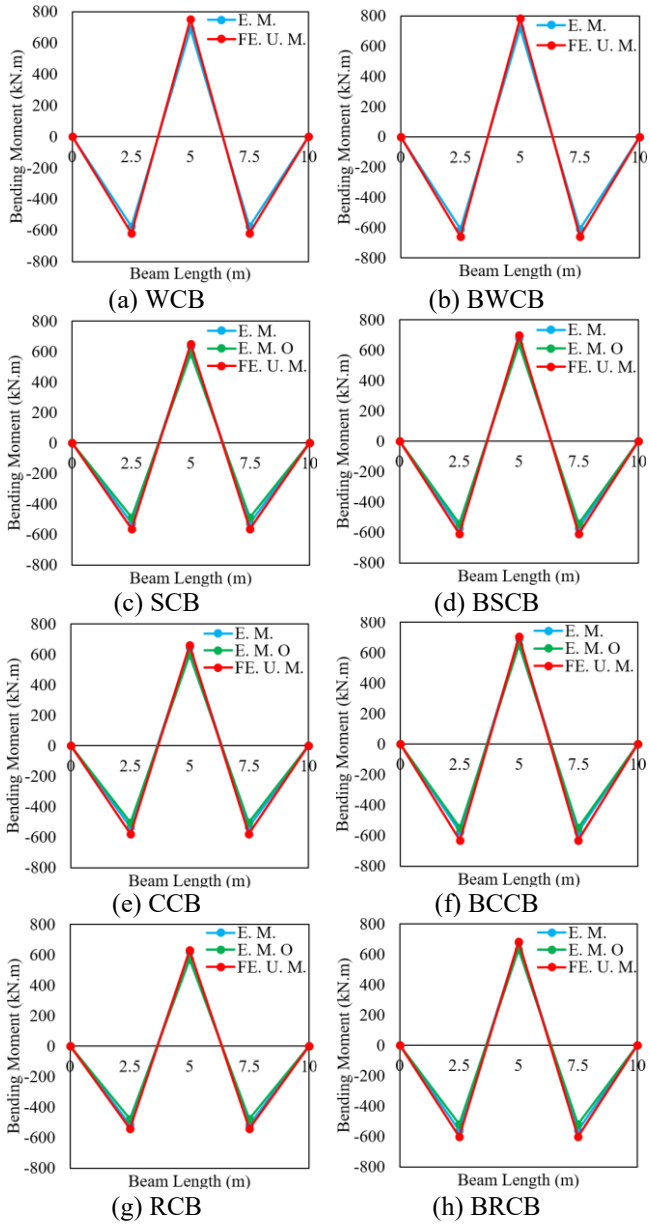

Figure 9. Bending moment distribution along the two spans of the continues composite beam

5.3 Moments redistribution

The redistribution of moments in the tested composite beam specimens was analyzed to evaluate the influence of web openings and BFRP strengthening on structural performance under ultimate loading. Two principal contributors to redistribution were considered: geometric discontinuities caused by web openings and material nonlinearity (plasticity). The redistribution factor (β) was calculated as the ratio of the moment difference between the elastic and ultimate states to the elastic moment, distinguishing between components attributed to openings and those due to plasticity.

From Table 4 and Figure 9, it can be shown that the reference specimen without any web opening (WCB) exhibited an ultimate load capacity of 460 kN and a total redistribution factor (β_{total}) of 0.06, entirely stemming from plastic deformation, indicating balanced load transfer without geometric disruptions. The BFRP-strengthened counterpart (BWCB) showed an increased ultimate load of 490 kN while maintaining the same β_{total} of 0.06, signifying that the preserved plastic redistribution capacity without adding

stiffness-related constraints.

Beams with web openings but without strengthening (SCB, CCB, RCB) demonstrated reduced load-carrying capacities (420, 430, and 410 kN, respectively) and elevated redistribution levels due to the introduction of stress concentrations and stiffness discontinuities. The redistribution attributed to openings ($\beta_{opening}$) for SCB, CCB, and RCB was 0.07, 0.06, and 0.09, respectively. Notably, the RCB specimen with a rectangular opening presented the highest total redistribution factor (β_{total} = 0.13), indicating that rectangular openings cause more severe stress imbalances than square or circular ones.

Beams with web openings strengthened by BFRP show considerable gain in strength as well as in redistribution behavior. The ultimate loads reached 455, 460, and 450 kN respectively. More importantly, the β opening values were reduced to 0.05 for BSCB, 0.04 for BCCB, and 0.07 for BRCB, indicating that BFRP restrains the adverse effects of redistribution which is normally accentuated by the openings. Minimum total redistribution was seen in BCCB (β_{total} = 0.09) highlighting circular openings along with wrapping by BFRP to restore stiffness and improve moment transfer.

It can be concluded that BFRP wrapping had a great role to play in reducing the moments that were getting redistributed due to web openings, especially in cases where geometry played a critical role. From these results, BFRP strengthening shows itself effective in keeping structural integrity while also boosting the performance of composite beams under ultimate loading conditions.

Table 4. Moment redistribution of selected beam specimens

Specimen	Ultimate Load Pu (kN)	Elastic Moment of Pu Without Opening (kNm)		Elastic Moment of Pu with Opening (kNm)		Ultimate Bending Moment (kNm)		β		
		Mid Span	Internal Support	Mid Span	Internal Support	Mid Span	Internal Support	Caused by Opening	Plasticity	In Total
WCB	460	575	690	—	—	620	750	—	0.06	0.06
SCB	420	525	635	490	585	565	650	0.07	0.05	0.12
CCB	430	535	645	505	595	580	660	0.06	0.05	0.11
RCB	410	515	620	475	570	540	630	0.09	0.04	0.13
BWCB	490	610	720	—	—	660	785	—	0.06	0.06
BSCB	455	570	680	540	640	610	700	0.05	0.05	0.1
BCCB	460	575	690	550	650	630	705	0.04	0.05	0.09
BRCB	450	560	675	520	630	600	685	0.07	0.04	0.11

6. STATISTICAL ANALYSIS

Web openings and material strengthening have been factors that play a crucial role in composite beams. Thus, a statistical analysis has been carried out in this section to study the effect of different shapes of web openings (square, circular, and rectangular) on moment redistribution and how effective BFRP reinforcing is in reducing these effects. Web openings create geometric discontinuities that lead to concentration of stress and moment redistribution inside the beam that can seemingly predispose it to fail when loaded. The application of BFRP strengthening serves to restore beam stiffness as well as correct moment redistribution.

This study uses stats to look at the final load limits and twisting actions of beams made with and without openings in the web, along with how BFRP support changes things. The redistribution factor (β) that shows changes in moment spread caused by openings and plasticity is checked out.

The effect percentage of BFRP on the ultimate load (P_u) is calculated using the following formula:

$$\text{Effect of BFRP on Ultimate Load (\%)} = \frac{P_{BFRP} - P_{\text{without BFRP}}}{\beta_{\text{without BFRP}}} \times 100\% \quad (6)$$

where, P_{BFRP} = Ultimate load for specimens with BFRP; $P_{\text{without BFRP}}$ = Ultimate load for specimens without BFRP. For example, for BWCB (BFRP on WCB):

$$\text{Effect of BFRP on Ultimate Load (\%)} = \frac{490-460}{460} \times 100\% = 605\% \quad (7)$$

The percentage of BFRP effect on the total redistribution factor (β_{total}) is calculated using the following formula:

$$\text{Effect of BFRP on Redistribution Factor (\%)} = \frac{\beta_{\text{without BFRP}} - \beta_{BFRP}}{\beta_{\text{without BFRP}}} \times 100\% \quad (8)$$

where, β_{BFRP} = Redistribution factor for specimens with BFRP; and $\beta_{\text{without BFRP}}$ = Redistribution factor for specimens without BFRP. For example, for BWCB (BFRP on WCB):

$$\text{Effect of BFRP on Redistribution Factor (\%)} = \frac{0.12-0.6}{0.12} \times 100\% = 50\% \quad (9)$$

The effect percentage of BFRP on the redistribution factor caused by opening ($\beta_{opening}$) is calculated using the following formula:

$$\text{Effect of BFRP on Opening Redistribution (\%)} = \frac{\beta_{\text{opening without BFRP}} - \beta_{\text{opening with BFRP}}}{\beta_{\text{opening without BFRP}}} \times 100\% \quad (10)$$

where, $\beta_{\text{opening with BFRP}}$ = Redistribution factor caused by the opening for specimens with BFRP; and $\beta_{\text{opening without BFRP}}$ = Redistribution factor caused by the opening for specimens without BFRP. For example, for BSCB (BFRP on SCB):

$$\text{Effect of BFRP on Opening Redistribution (\%)} = \frac{0.07-0.05}{0.07} \times 100\% = 28.57\% \quad (11)$$

The results, summarized in Table 5, provide insight into how BFRP strengthening helps to mitigate the negative impact of web openings, enhancing both structural integrity and overall performance.

Table 5. Statistical analysis of moment redistribution in composite beams with web openings and BFRP strengthening

Specimen	Ultimate Load P_u (kN)	Effect of BFRP on P_u (%)	Redistribution Factor (β_{total})	Effect of BFRP on β_{total} (%)	Redistribution Factor ($\beta_{opening}$)	Effect of BFRP on $\beta_{opening}$ (%)
WCB	460	-	0.06	-	N/A	N/A
SCB	420	-	0.12	-	0.07	-
CCB	430	-	0.11	-	0.06	-
RCB	410	-	0.13	-	0.09	-
BWCB	490	6.50%	0.06	50%	N/A	N/A
BSCB	455	8.33%	0.1	16.67%	0.05	28.57%
BCCB	460	7.00%	0.09	18.18%	0.04	33.33%
BRCB	450	9.80%	0.11	15.38%	0.07	22.22%

The application of BFRP strengthening has been proved to advance, in a very significant way, the structural performance of composite beams with web openings. This stands true for both ultimate load capacity and moments redistribution behavior. Beams reinforced with BFRP show an enhancement in load-carrying capacity under all ascertained modalities, wherein rectangular opened beams gain maximum benefaction. For example, the RCB specimen exhibited a 9.8% increase in ultimate load from 410 kN to 450 kN. This was the highest witnessed increment among the different beam configurations and thus indicates that BFRP tends to improve beam strength most when there are rectangular web openings.

BFRP significantly reduces the redistribution factor (β_{total}), along with enhancing the ultimate load, a measure of moment redistribution within the beam. BFRP coating reduces the redistribution factor, thereby improving moment transfer behavior at the beam. This is demonstrated by the fact that the BWCB specimen exhibited no web openings and recorded a maximum reduction of 50% in redistribution factors (0.12 to 0.06). Thus, BFRP not only increases the beam's load-bearing capacity but also introduces efficient moment distribution. For other specimens, such as SCB-BFRP, the reduction was more modest at 16.67% (from 0.12 to 0.10), indicating that BFRP still has a beneficial effect, albeit to a lesser extent when web openings are present.

Another key part of the research was the redistribution resulting from the web opening itself ($\beta_{opening}$), which BFRP has demonstrated can significantly mitigate the effects of redistribution resulting from web openings. The BCCB specimen with circular openings showed a significant 33.33% reduction in opening-related redistribution, decreasing from 0.06 to 0.04. The BRCB specimen with RCB also showed a further significant 22.22% reduction in opening-related redistribution. These results once again substantiate the claim that BFRP has the potential to reduce the negative effects of openings on the structural performance of composite beams, particularly those with circular and rectangular openings, where this effect is most pronounced.

Overall, the results prove that BFRP strengthening has a very major effect on increasing ultimate load capacity and moment redistribution while minimizing the effects of openings on structural response for continuous beams with different web openings. The RCB and BCCB specimens exhibited maximum enhancement which highlights the role of BFRP in restoring beam stiffness and strength under complicated loading conditions.

7. CONCLUSIONS

This paper investigated the nonlinear structural behavior of continuous composite beams with different web opening shapes (square, circular, and rectangular), unstrengthened and strengthened externally with BFRP wrapping. The main aim was to see how web openings affect deflection, shear, moment redistribution and final load capacity as well as to check BFRP's effectiveness in restoring and improving structural performance. The major conclusions are:

a. Web openings increased mid-span deflection due to local stiffness reduction; rectangular openings produced the maximum deflection increase 45% compared to intact beams. BFRP wrapping significantly mitigated this increase, with maximum deflection reductions of 20–30%, particularly in cases with rectangular and square openings.

b. Shear stress concentrations were elevated in rectangular configurations (60% with respect to intact beams). BFRP application shear flow redistribution gave lower peak stresses by up to 40%, hence improved shear performance and reduced failure risk.

c. Rectangular openings appeared with $\beta_{total} = 0.13$. BFRP wrapping reduced the redistribution demands, it reduced βopening by 28.6% in square openings, 33.3% in circular openings, and 22.2% in rectangular ones. Circular openings plus BFRP wrapping showed the lowest total redistribution $\beta_{total} = 0.09$ and thus presented an ideal balance between shape and strengthening efficiency.

d. Web opening led to a reduction in ultimate load capacity by as much as 10.9%, BFRP wrapping however restored most of this capacity with increment of 8.3% in BSCB, 7.0% in BCCB and 9.8% in BRCB noted. The maximum ultimate capacity attained was 490 kN and it was registered by the BFRP-strengthened beam without openings (BWCB). Also, the strengthened beam with rectangular openings reached only 450 kN.

e. Analytical model founded on an improved strut-and-tie technique and shows high accuracy and dependability. It successfully forecasts the final strength of shear of selected beams, both unblemished and subjected to maximum loads with very little error (3%) from numerical outcomes.

f. Statistical analysis corroborates that BFRP strengthening causes a substantial enhancement of structural performance in beams with web openings. Redistribution factors due to geometric discontinuities were mitigated by as much as 33.3% for BCCB and total redistribution was maximally reduced in BWCB. The redistribution factor for the reference beam WCB was 0.06, strengthening the case that strengthening preserved ductility and did not alter the internal load path.

The analytical, numerical, and statistical assessments carried out prove that BFRP wrapping is a valid rehabilitation method for web-opened reinforced concrete beams. It increases strength, controls deformation, provides lower stress concentration values, and improves moment redistribution behavior significantly. Such results give important design guidance for structural engineers when facing performance

challenges in opening-bearing beams commonly found in retrofit applications and resilience-driven applications.

REFERENCES

[1] Friedman, A. (2023). Utilities systems for sustainability. In Fundamentals of Innovative Sustainable Homes Design and Construction, pp. 177-201. https://doi.org/10.1007/978-3-031-35368-0_7

[2] El-Kareim, A., Arafa, A., Hassanin, A., Atef, M., Saber, A. (2020). Behavior and strength of reinforced concrete flanged deep beams with web openings. Structures, 27: 506-524. https://doi.org/10.1016/j.istruc.2020.06.003

[3] Al-Dafafea, T., Durif, S., Bouchaïr, A., Fournely, E. (2019). Experimental study of beams with stiffened large web openings. Journal of Constructional Steel Research, 154: 149-160. https://doi.org/10.1016/j.jcsr.2018.11.026

[4] Hashim, N.S., De'nan, F. (2024). The magnitude of stress concentration of I-beam with web opening because of lateral-torsional buckling effects. World Journal of Engineering, 21(2): 386-397. https://doi.org/10.1108/WJE-06-2022-0234

[5] Luo, Z., Shi, Y., Xue, X., Li, H. (2025). Design recommendations for web-opened titanium-clad bimetallic steel plate girders under patch loading. Journal of Structural Engineering, 151(2): 04024211. https://doi.org/10.1061/JSENDH.STENG-13901

[6] Abdel-Kareem, A.H. (2014). Shear strengthening of reinforced concrete beams with rectangular web openings by FRP Composites. Advances in Concrete Construction, 2(4): 281. https://doi.org/10.12989/acc.2014.2.4.281

[7] Sayed, A.M. (2019). Numerical study using FE simulation on rectangular RC beams with vertical circular web openings in the shear zones. Engineering Structures, 198: 109471. https://doi.org/10.1016/j.engstruct.2019.109471

[8] Elansary, A.A., Aty, A.A.A., Abdalla, H.A., Zawam, M. (2022). Shear behavior of reinforced concrete beams with web opening near supports. Structures, 37: 1033-1041. https://doi.org/10.1016/j.istruc.2022.01.040

[9] Meng, B., Xiong, Y., Zhong, W., Duan, S., Li, H. (2023). Progressive collapse behaviour of composite substructure with large rectangular beam-web openings. Engineering Structures, 295: 116861. https://doi.org/10.1016/j.engstruct.2023.116861

[10] Ahmed, A., Fayyadh, M.M., Naganathan, S., Nasharuddin, K. (2012). Reinforced concrete beams with web openings: A state of the art review. Materials and Design, 40: 90-102. https://doi.org/10.1016/j.matdes.2012.03.001

[11] Salih, R., Abbas, N., Zhou, F. (2021). Experimental and numerical investigations on the cyclic load behavior of beams with rectangular web openings strengthened using FRP sheets. Structures, 33: 655-677. https://doi.org/10.1016/j.istruc.2021.04.051

[12] Abbas, O.H., Numan, H.A. (2021). A state of the art review on transverse web opening for reinforced concrete beams with and without strengthening method. Journal of Physics: Conference Series, 1895(1): 012059. https://doi.org/10.1088/1742-6596/1895/1/012059

[13] Tsavdaridis, K.D., D'Mello, C. (2012). Optimization of novel elliptically-based web opening shapes of perforated steel beams. Journal of Constructional Steel Research, 76: 39-53. https://doi.org/10.1016/j.jcsr.2012.03.026

[14] Hashim, N.S., De'nan, F. (2024). The numerical assessment of stress distribution of I-beam with web opening. World Journal of Engineering, 21(5): 986-1001. https://doi.org/10.1108/WJE-03-2023-0078

[15] Galustanian, N., El-Sisi, A., Amer, A., Elshamy, E., Hassan, H. (2023). Review of the structural performance of beams and beam–column joints with openings. CivilEng, 4(4): 1233-1242. https://doi.org/10.3390/civileng4040068

[16] Altaee, M.J., Cunningham, L.S., Gillie, M. (2017). Experimental investigation of CFRP-strengthened steel beams with web openings. Journal of Constructional Steel Research, 138: 750-760. https://doi.org/10.1016/j.jcsr.2017.08.023

[17] Altaee, M.J.M. (2019). CFRP Strengthening of steel beams with web openings. Doctoral dissertation. The University of Manchester (United Kingdom).

[18] Abdulrahman, B.Q. (2024). GFRP continuous RC beams having web openings and externally strengthened with CFRP composites. Engineering Research Express, 6(1): 015089. https://doi.org/10.1088/2631-8695/ad26dc

[19] Kumari, A., Nayak, A.N. (2021). An experimental approach for strengthening of RC deep beams with web openings using GFRP fabrics and gas actuated fasteners. Journal of Building Engineering, 35: 102027. https://doi.org/10.1016/j.jobe.2020.102027

[20] Shehab, E.Q., Riyadh, A. (2025). A new approach to sustainable environmental assessment for wastewater treatment plants-A case study in the central region of Iraq. Ecological Engineering and Environmental Technology, 26(1): 124-136. https://doi.org/10.12912/27197050/194126

[21] Özkılıç, Y.O., Aksoylu, C., Gemi, L., Arslan, M.H. (2022). Behavior of CFRP-strengthened RC beams with circular web openings in shear zones: Numerical study. Structures, 41: 1369-1389. https://doi.org/10.1016/j.istruc.2022.05.061

[22] Jasim, W.A., Tahnat, Y.B.A., Halahla, A.M. (2020). Behavior of reinforced concrete deep beam with web openings strengthened with (CFRP) sheet. Structures, 26: 785-800. https://doi.org/10.1016/j.istruc.2020.05.003

[23] Sharma, P. (2016). An introduction to Basalt rock fiber and comparative analysis of engineering properties of BRF and other natural composites. International Journal for Research in Applied Science and Engineering Technology, 4(1): 141-148.

[24] Pavlović, A., Donchev, T., Petkova, D., Staletović, N. (2022). Sustainability of alternative reinforcement for concrete structures: Life cycle assessment of Basalt FRP bars. Construction and Building Materials, 334: 127424. https://doi.org/10.1016/j.conbuildmat.2022.127424

[25] Alsultani, R., Karim, I.R., Khassaf, S.I. (2025). Experimental and numerical investigation into pile spacing effects on the dynamic response of coastal pile foundation bridges considering current-wave-earthquake forces. Advances in Bridge Engineering, 6: 1. https://doi.org/10.1186/s43251-024-00147-z

[26] Duan, S.J., Feng, R.M., Yuan, X.Y., Song, L.T., Tong, G.S., Tong, J.Z. (2025). A review on research advances and applications of Basalt Fiber-Reinforced Polymer in

the construction industry. Buildings, 15(2): 181. https://doi.org/10.3390/buildings15020181

[27] Joudah, Z.H., Hafizah, A., Khalid, N., Algaifi, H.A., Mhaya, A.M., Xiong, T., Huseien, G.F. (2024). Effects of waste glass bottle nanoparticles and high volume of waste ceramic tiles on concrete performance when exposed to elevated temperatures: Experimental and theoretical evaluations. Fire, 7(12): 426. https://doi.org/10.3390/fire7120426

[28] Riyadh, A., Saber, Q., Al-Saadi, A., Mohammed, O., Abed, S., Naser, R., Hussein, A., Muslim, F., Fadhil, H., Karim, I., Khassaf, S. (2024). The impact of climate change on the reinforcement durability of concrete bridge structures. The Open Civil Engineering Journal, 18: e18741495337012. http://doi.org/10.2174/0118741495337012240812105905

[29] Li, L., Liao, W., Wang, J., Zhou, D. (2015). Behavior of continuous steel-concrete composite beams with web openings. International Journal of Steel Structures, 15(4): 989-997. https://doi.org/10.1007/s13296-015-1218-2

[30] Ollgaard, J.G., Slutter, R.G., Fisher, J.W. (1971). Shear strength of stud connectors in lightweight and normal weight concrete. Engineering Journal, 8(2): 55-64. https://doi.org/10.62913/engj.v8i2.160

[31] Saber, Q.A., Alsultani, R., Al-Saadi, A.A., Karim, I.R., Khassaf, S.I., Mohammed, O.I., Abed, S.M., Naser, R.A., Hussein, A., Muslim, F., Naimi, S., Salahaldain, Z. (2025). Structural finite element analysis of bridge piers with consideration of hydrodynamic forces and earthquake effects for a sustainable approach. Mathematical Modelling of Engineering Problems, 12(3): 1071-1080. https://doi.org/10.18280/mmep.120334

[32] El-Demerdash, W.E., El-Metwally, S.E., El-Zoughiby, M.E., Ghaleb, A.A. (2016). Behavior of RC shallow and deep beams with openings via the strut-and-tie model method and nonlinear finite element. Arabian Journal for Science and Engineering, 41: 401-424. https://doi.org/10.1007/s13369-015-1678-x

[33] Lanes, R.M., Greco, M., Guerra, M.B.F. (2019). Strut-and-tie models for linear and nonlinear behavior of concrete based on topological evolutionary structure optimization (ESO). Revista IBRACON de Estruturas e Materiais, 12(1): 87-100. https://doi.org/10.1590/S1983-41952019000100008

[34] Mageed, N.N., Al-Sultani, R., Abbas, A.W.N. (2024). The impact of using advanced technologies in sustainable design to enhance usability and achieve optimal architectural design. International Journal of Sustainable Development and Planning, 19(11): 4273-4280. https://doi.org/10.18280/ijsdp.191116

[35] Carvalho, L., Pimentel, M., Arêde, A., Pouca, N.V., Degaldo, P., Pinto, J.R. (2023). Design of pre-cast two-column bents using strut-and-tie models and nonlinear finite element analysis. In International Symposium of the International Federation for Structural Concrete, pp. 1732-1741. https://doi.org/10.1007/978-3-031-32519-9_174

[36] Russo, S. (2016). First investigation on mixed cracks and failure modes in multi-bolted FRP plates. Composite Structures, 154: 17-30. https://doi.org/10.1016/j.compstruct.2016.07.016